Study on Continuous Catalyst Reformer and Catalyst Regeneration Process

by

Nagentheran A/L Subramaniam

Dissertation submitted in partial fulfillment of

the requirements for the

Bachelor of Engineering (Hons)

Chemical Engineering

JANUARY 2009

Universiti Teknologi PETRONAS

Bandar Seri Iskandar

31750 Tronoh

Perak Darul Ridzuan
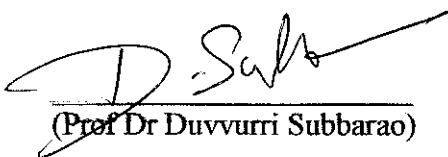
CERTIFICATION OF APPROVAL

Study on Continuous Catalytic Reformer and Catalyst Regeneration Process

by

Nagentheran A/L Subramaniam

A project dissertation submitted to the

Chemical Engineering Programme

Universiti Teknologi PETRONAS

in partial fulfilment of the requirement for the

BACHELOR OF ENGINEERING (Hons)

(CHEMICAL ENGINEERING)

Approved by,
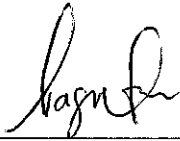
_____
(Prof Dr Duvvurri Subbarao)

UNIVERSITI TEKNOLOGI PETRONAS

TRONOH, PERAK

January 2009

i

CERTIFICATION OF ORIGINALITY

This is to certify that I am responsible for the work submitted in this project, that the original work is my own except as specified in the references and acknowledgements, and that the original work contained herein have not been undertaken or done by unspecified sources or persons.

<u>NAGENTHERAN A/L SUBRAMANIAM</u>

ABSTRACT

Regeneration of coked catalyst in a naphtha reformer is studied based on the effectiveness of rate coke burn off. Catalyst is temporarily deactivated by the coke deposits which are burnt in the regeneration for the catalyst reactivation. Catalyst gets deactivated by coke deposition blocking the active sites and reduces the selectivity of catalyst and the products yields. For predicting the behavior subject to catalyst deactivation, coking rate equation and the kinetic model is obtained. All reformers are moving bed and radial flow reactors. The coked catalyst are moved continuously and slowly from the reactors, withdrawn from the last reactor regenerated in a regeneration section and returned to first reactor as fresh catalyst. Coke content on the catalyst increases with residence time of catalyst. Catalyst deactivation is directly proportional to the amount of coke deposits on the catalyst. To understand and contribute to this problem, a modeling of the regeneration of coked catalyst particles (Pt-Al$_2$O$_3$) are used as model catalyst to (1) determine of the intrinsic and effective kinetics of coke burn-off (2) characterization of the catalyst's on influence of the temperature on the pore effectiveness factor, rate of mass transfer, and reactivity of coked catalyst (3) Influence of carbon load on porosity and tortuosity of the catalyst. With this information, modeling of the coked catalyst regeneration is produced.

ACKNOWLEDGEMENT

TABLE OF CONTENTS

LIST OF FIGURES

LIST OF TABLES

CHAPTER 1

INTRODUCTION

1.1 BACKGROUND

Continuous Catalyst Regeneration (CCR) process is part of a process used in the petroleum and petrochemical industries, which produces aromatics from naphthenes and paraffin's commonly used as motor fuel. The continuous catalytic regeneration of fluidized catalyst cracker has been the subject of many developments in the past, resulting in the construction of smaller regenerators, with lower catalyst inventories, operating at higher temperatures. The reduction in catalyst hold-up permits catalyst to be replaced faster through regular catalyst addition and withdrawal. The biggest development in catalyst regeneration was the use of CO combustion promoter. This allowed better control of the regenerator temperature and improved flexibility of operation in terms of air consumption and flue gas composition. This kind of process is used when the catalyst maintains its activity sufficiently long, for several months or a year or two as in the cases of some catalytic reforming processes. A few processes have operated on cycles of reaction and regeneration of less than an hour or a few hours. A minimum of three vessels usually is needed: One on-stream, one being regenerated, and the last being purged and prepared for the next cycle. Because the catalyst degrades in a few minutes, it is circulated continuously between reaction and regeneration zones. Reforming reactions occur in chloride promoted fixed catalyst beds; or continuous catalyst regeneration (CCR) beds where the catalyst is transferred from one stage to another, through a catalyst regenerator and back again.

1.2   PROBLEM STATEMENT

Catalyst coked is a common problem. With porous solids, this can take the form of pore blockage, which effectively prevents access to the majority of active sites, ultimately restricting the chemistry to the external surface. This can take the form of 'coking', although this tends to be less of a problem in liquid phase reactions than in the higher temperature gas phase reactions. Coke formation can be removed carefully burning it in an air-nitrogen mixture. Reversible deactivation can be corrected by regeneration of coking, improper chloride level, platinum agglomeration, carbon monoxide poisoning and sulphur or nitrogen poisoning.

However, there is limitation in regeneration process which some process cannot correct irreversible deactivation such a poisoning from heavy metals example sodium, lead, arsenic etc and also surface area loss from overheating or normal ageing.

1.3 OBJECTIVES AND SCOPE OF PROJECT

- ➢ To do case study on continuous catalytic reformer (CCR) and catalytic regeneration process implemented in petroleum refinery.
- ➢ To do modeling of regeneration of coked catalyst and verification of coke burn-off in single particles and fixed bed reactors.

CHAPTER 2

LITERATURE REVIEW

Catalytic reforming of naphtha or mixture of naphtha with a certain amount of cracking oil is a process of great interest to the petrochemical industry for the production of aromatic compounds that are raw materials for plastics, elastomers and resins manufacture. Catalytic reforming unit uses naphtha or cracking oil as feedstock to produce rich aromatic compounds and high octane value liquid products through reactions such as aromatization, cyclization, and hydro cracking. At the same time, it produces hydrogen (H) and liquefied petroleum gas (LPG) as its by-products. The design or simulation of the catalytic reforming reactor is very difficult because of complicated components of catalytic reforming feedstock, higher operating temperature of the system, and the complicated reactions in the reactor. In several refinery and petrochemical processes the catalyst deactivates by coke formation, e.g. during cracking of heavy oil, hydrodesulphurization and reforming of naphtha into high octane gasoline. The catalyst must be regenerated by continuous or periodic coke combustion. In case of a fixed bed reactor, the regeneration procedure is conducted periodically after a certain time of operation, i.e., the reactor is shut down for burn-off. During this non-steady state, process precautions have to be taken to avoid excessive high temperatures, e.g. in case of naphtha reforming the Pt–Al2O3-catalyst, the latter loses surface and mechanical resistance beyond temperatures of 550 °C. So the air is strongly diluted with nitrogen to avoid damage to the catalyst.

Regeneration can normally be improved by increasing catalyst bed level (inventory) or by increasing regenerator temperature (e.g., increasing catalyst makeup rate, activity). In complete combustion, increased air results in lower regenerator

temperature (since there is no more CO to burn), the extra gas volume removes heat). In partial combustion of course, increased air will increase regenerator temperature. Complete CO combustion requires more air to burn the same amount of coke due to the excess oxygen in the flue gas. The CO must be eliminated from the dilute phase to control afterburning and avoid hot cyclones.

By increasing the promoter activity, after burn can be controlled, but at some point adding more promoters will have no effect. Over promotion may even lead to local oxygen depletion, and will generate more NO_x. CO promotion performance of the unit's circulating catalyst can be tested in the laboratory, but provides only relative combustion activity. In case of doubt, a quick check is made by adding a batch of new promoter to the regenerator and watching the response of the regenerator bed and flue gas temperatures. A conventional naphtha catalytic reforming unit consists of 3 or 4 radial flow reactors in series operated under adiabatic conditions. The temperature and the H2/HC molar ratio are the most important process variables. Reaction rates were derived from the assumption of a homogeneous system.
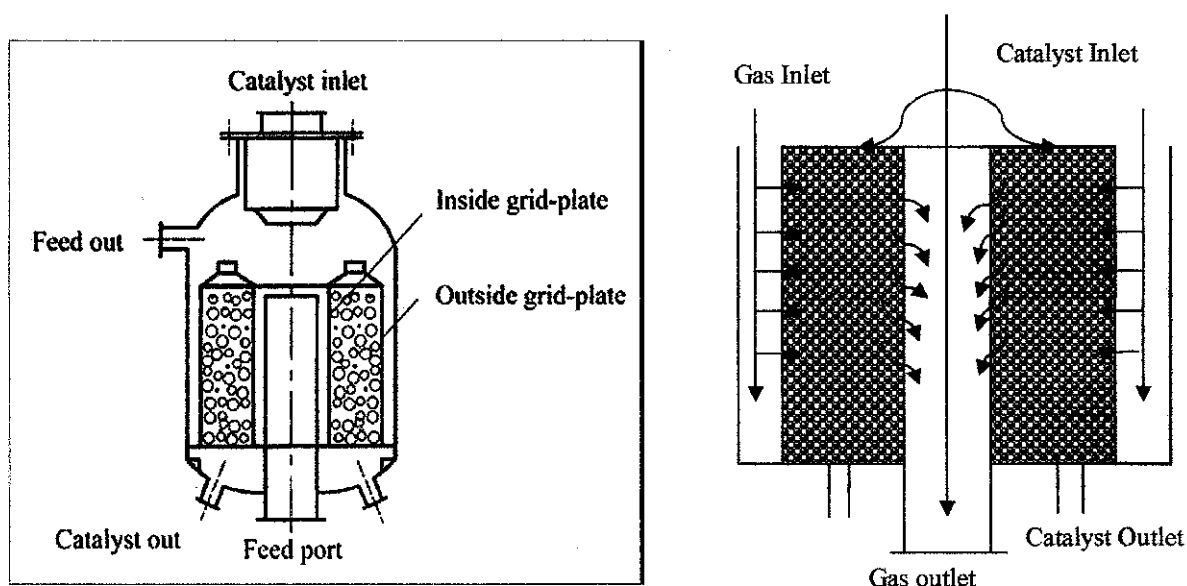
FIGURE 1.0: CONTINUOUS CATALYTIC REFORMER

Industrial catalysts used in recent catalytic reforming units are consisted of Gama Alumina support, metals such as Platinum, Rhenium, Germanium, and Iridium, less than one weight percent, and additives such as chlorine to increase isomerisation reactions. On the other hand, coke formation and coke deposition, causing the deactivation of the catalyst, are undesired reactions.

Certain petroleum refining processes, such as catalytic cracking, catalytic reforming, isomerisation, etc. are carried out at elevated temperatures in the presence of a catalyst. In some of these processes coking of the catalyst occurs, i.e. coke is deposited onto the catalyst, with the result that over a period of time the catalyst gradually loses its activity. To restore the activity of the catalyst, the catalyst must be periodically regenerated, which is usually accomplished by combusting the coke at elevated temperatures in the presence of an oxygen-containing gas, such as air or oxygen-enriched air. The catalytic process may be carried out by any one of various procedures; e.g. it may be a fixed bed process, in which case the catalytic reaction and catalyst regeneration are conducted in a single vessel, or it may be one of the moving catalyst processes, such as a transport bed process or a fluidized bed process, in which case the catalytic reaction is carried out in one vessel and catalyst regeneration is carried out in another vessel. A major advantage that moving catalyst processes have over fixed bed processes is that in moving bed processes, the reaction can be carried out continuously, whereas in fixed bed processes, the catalytic reaction must be terminated periodically to regenerate the catalyst.

In moving catalyst systems, the hydrocarbon feed and hot freshly regenerated catalyst, and perhaps steam, is continuously introduced into the reactor. The hot catalyst causes the hydrocarbon feed to react, thereby producing an array of valuable hydrocarbon products which may be of lower molecular weight than the hydrocarbon feed. During the course of the reaction the catalyst becomes fouled with coke deposits and loses its catalytic activity. The hydrocarbon products and fouled catalyst are separated and each leaves the reactor; the hydrocarbon products being sent to downstream hydrocarbon separation units to recover the various products, and the

fouled catalyst being transported to a catalyst regenerator for removal of coke from the catalyst. The effectiveness of the regenerator in burning coke off the catalyst directly determines the quality of performance of the hydrocarbon reaction (e.g. cracking) step. The regeneration step provides reactivated catalyst and heat for the endothermic hydrocarbon cracking step. The catalyst is heated during the regeneration step and the hot catalyst is transported to the reactor, where it contacts the hydrocarbon feed and causes the reactions to occur.

The amount of oxygen-containing gas (e.g. air) present in the regenerator determines the amount of coke that can be burned off the catalyst. The kinetics and efficiency of the combustion process also determines the steady-state concentrations of coke returned to the reactor on the reactivated catalyst, and the amount of coke on the spent catalyst entering the regenerator. In general, the more efficiently the catalyst is reactivated, the better its hydrocarbon reaction activity and selectivity will be, and the greater its ability to process heavier, poorer quality feedstock will be. The rate of coke combustion is usually controlled by regulating the amount of oxygen entering the coke combustion zone during catalyst regeneration. Traditionally, catalyst regeneration has been carried out using air as the oxygen-containing gas.

The nitrogen in air serves to remove heat from the reaction zone, thereby moderating the combustion. If it is desired to increase the rate of combustion, the flow of air through the regeneration zone is increased. This will have the sometimes undesirable effect of increasing the velocity of gas flowing through the combustion zone, which can cause excessive attrition and loss of the catalyst and excessive wear on equipment. To avoid these effects, some recent improvements have centered on the use of other oxygen-inert gas mixtures, such as oxygen-carbon dioxide mixtures for catalyst regeneration. Carbon dioxide has a greater heat capacity than nitrogen; accordingly the same amount of heat transfer can be affected with a lower volume of carbon dioxide than would be required using nitrogen, which means that the feed gas can be richer in oxygen. In the case of continuous regeneration processes, such as fluidized catalytic

cracking, this provides an additional advantage in that additional hydrocarbon can be processed in a cracking reactor of given size.

One of the difficulties associated with the use of oxygen-carbon dioxide mixtures is providing sources of oxygen and carbon dioxide. Oxygen can be easily generated by an on-site oxygen generator. The viability of an oxygen carbon dioxide-based regeneration process is determined by the ability to obtain carbon dioxide economically. Carbon dioxide can also be provided by recycling carbon dioxide produced during the combustion of the coke deposits.

The above-described prior art references discuss the operation of decoking processes using mixtures of pure oxygen and carbon dioxide, but none of the references discuss the most important aspect, i.e. how the operating mixture of oxygen and carbon dioxide is initially attained. This provides an efficient and economical method of starting up an oxygen and carbon dioxide-based catalyst decoking process.

CHAPTER 3

METHODOLOGY

The aims of this work to study and make the modeling of the decoking processes of coke burn-off within a single particle and regeneration of a coked fixed bed. Based on study and research carried out under typical industrial conditions, a selection of adequate analytical techniques for intrinsic kinetics of coke burn-off is taken account. The strategy used for this research includes six steps:

- ➢ Research and study.
- ➢ Analytical part.
- ➢ Construction of kinetic expressions.
- ➢ Evaluation of inhibition effects.
- ➢ Modeling of coke burn-off within a single particle and modeling of regeneration in a fixed bed reactor.

Table 1.0: Gantt chart of Final Year Project

		1	2	3	4	5	6	7	8	9	10	11	12	13	14	15	16
1	Selection of project title	■															
2	Preliminary research work		■	■													
3	Submission of preliminary report				■												
4	Seminar(optional)					■	■										
5	Project work					■	■										
6	Submission of progress report									■							
7	Seminar 2 (compulsory)										■	■	■	■			
8	Project work continues									■	■	■	■	■			
9	Submission of interim report final draft															■	
10	Oral presentation																■

CHAPTER 4

THEORY

4.1 INTRA-PARTICLE TRANSPORT MECHANISMS

Depending on the structure of the adsorbent, different types of diffusion mechanism become dominant and they can interact in different ways; these mechanisms are: pore diffusion, solid diffusion and reaction kinetics at phase boundaries.

In this case, *molecular diffusion* or *Knudsen diffusion* takes place, because the interaction between the molecules and the pore walls plays a crucial role (Russ, 2004). Knudsen diffusion occurs when the mean free path is relatively long compared to the pore diameter, so the molecules collide frequently with the pore wall.

In contrast with gas flow within the pore, there is the possibility of direct contribution to the flux from transport through the adsorbed layer on the surface of the macro pores; this kind of mechanism is called *surface diffusion* (Ruthven, 1984; p. 137).

4.2 MACRO PORE DIFFUSION

The effective macro pore diffusivity is a complex quantity, which includes contributions from one or more mechanisms (Ruthven, 1984). The contribution of the different mechanisms will depend mainly on the structure of the pores.

In macro pore diffusion the Fick's Law can be written as:

$$J = -\varepsilon_p D_p \frac{\partial c}{\partial z}$$

c concentration in gas phase within the macro pores

D_p pore diffusivity

J molar flux

ε_p particle porosity

The effects of the random orientation of the pores and their diameter variation reduce the pore diffusivity. This effect is usually accounted as a *tortuosity factor*. Since adsorption in the macro pores may be limited by molecular or Knudsen diffusion, a brief description of this type of diffusion follows.

4.3   MOLECULAR DIFFUSION

If transport within the pores occurs only by molecular diffusion, the pore diffusivity is given by:

$$D_p = \frac{D_m}{\tau}$$

D_m molecular diffusivity

D_p pore diffusivity

τ tortuosity factor

The molecular diffusivity for gaseous systems may be estimated with the Chapman-Enskog equation (Bird, 2002; p. 526).

$$D_m = \frac{0,001858 T^{3/2} \left(\dfrac{1}{Mw_i} + \dfrac{1}{Mw_j} \right)^{1/2}}{P \sigma_{ij}^{2} \Omega_{D,ij}}$$

Mw_i, Mw_j molecular weight of species i, j (kg/kmol)

P total pressure [Pa].

T temperature [K]

σ_{ij}: $\frac{1}{2}(\sigma_i + \sigma_j)$ collision diameter from the Lennard Jones potential [Angstroms]

$\Omega_{D,ij}$ collision integral for diffusion, a function of ε/kT

k Boltzmann constant

ε ($\varepsilon 1^*\varepsilon 2$) Lennard-Jones force constant [-]

4.4   KNUDSEN DIFFUSION

This kind of diffusion occurs when the collisions between gas molecules and pore walls become more dominant than collision between molecules, which are dominant in molecular diffusion. Therefore by colliding with the wall, a molecule loses its momentum in the direction of the pore and the more frequently a collision takes place the slower the diffusivity speed would be.

The Knudsen Diffusivity may be estimated by (Ruthven, 1984):

$$D_{ki} = 0.97 \frac{d_p}{2} \sqrt{\frac{T}{Mw_i}}$$

d_p equivalent pore diameter [m]

D_{ki} Knudsen diffusivity [m^2/s]

Mw_i molecular weight [kg/kmol]

T temperature [K]

The pore diffusivity is then calculated with the Bonsaquet equation, where the effect of both resistances is additive:

$$\frac{1}{D_p} = \tau_p \left(\frac{1}{D_{m,i}} + \frac{1}{D_{k,i}} \right)$$

$D_{k,i}$ Knudsen diffusivity both of component i in the mixture

D_p pore diffusivity

$D_{m,i}$ molecular diffusivity

τ Pore tortuosity factor (experimental: $2 < \tau < 6$; Ruthven; p. 134)

The appropriate dimensionless group characterizing film mass transfer is the Sherwood number, according to the correlation of Wakao and Funazkri (Wakao, 1978) defined as:

$$Sh_i = \frac{k_{fi} d_p}{D_{m,i}} = 2{,}0 + 1{,}1 Sc^{1/3} Re^{0,6}$$

d_p equivalent diameter

D_{mi} molecular diffusivity

k_{fi} film mass transfer coefficient

Re Reynolds number

Sc: Schmidt number

Sh_i Sherwood number

Dimensionless number defined as:

Microporous

R

External Fluid Film

$$Re = \frac{\rho_g u_g d_p}{\mu_g}$$

$$Sc_i = \frac{\mu_g}{\rho_g D_{mi}}$$
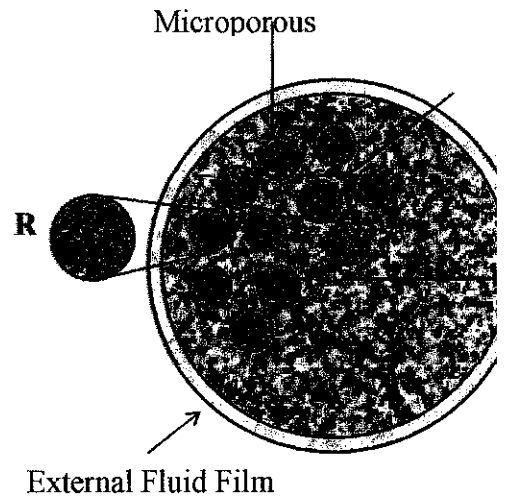
4.5 RATE COEFFICIENTS

Mechanism	Pore Diffusion	Solid Diffusion	External Film
Rate coefficient, k_r	$k = \dfrac{15(1-\varepsilon_b)\varepsilon_p D_{pi}}{r_p^{\,2}}$	$k = \dfrac{15 D_{ci}}{r_c^{\,2}}$	$k = \dfrac{3(1-\varepsilon_b)k_{f_z}}{\rho_b r_p}$

D_{ci} crystal diffusivity, [m²/s]

D_{pi} pore diffusivity [m²/s]

k_{fe} external mass transfer coefficient, [m/s]

r_c crystal radius, [m]

r_p particle radius, [m]

ε_b bed porosity, [-]

ε_p particle porosity [-]

ρ_b bed density [kg/m³]

- 12 -

4.6 AXIAL HEAT CONDUCTION AND HEAT TRANSFER

The *thermal dispersion term* in a non-isothermal adsorption process is represented, in analogy with the mass axial dispersion, as:

$$-\varepsilon_b \lambda_{ax} \frac{\partial^2 T_g}{\partial z^2}$$

T_g gas temperature

ε_b bed porosity

λ_{ax} effective axial thermal conductivity

Thus:

$$D_{ax} = a_{ax} = \frac{\lambda_{ax}}{\rho_g Cp_g}$$

a_{ax} thermal axial dispersion coefficient

Cp_g heat capacity of the gas

ρ_g gas density

The heat transfer between the gas and the bed can be represented as:

$$Q_{gs} = \alpha_{gs} A_{sp} \left(T_g - T_s \right)$$

A_{sp} macroscopic particle surface per bed volume

Q_{gs} heat transfer between solid and gas phase

T_s solid temperature

α_{gs} heat transfer coefficient between solid and gas phase

In order to determine the heat transfer parameters in the packed bed, it is assumed that the convective transport of heat and mass occur by the same mechanism, since the radiation contribution can be neglected at typical temperatures encountered (Ruthven, 1984; p. 216).

$$Nu = \frac{\alpha_{gs} d_p}{\lambda_g} \equiv Sh = \frac{k_f d_p}{D_m}$$

$$\Pr = \frac{C_{pg} \mu_g}{\lambda_g} \equiv Sc = \frac{\mu_g}{\rho_g D_m}$$

d_p equivalent particle diameter ,

k_f film mass transfer coefficient

Nu Nusselt number

Pr Prandtl Number

$Sext$ macroscopic particle surface

$Vext$ macroscopic particle volume

λ_g thermal conductivity of the gas

μ_g gas viscosity

The fluid particle gas transfer coefficient is given by (Ruthven, 1984; p. 216):

$$Nu = 2,0 + 1,1 \operatorname{Re}^{0,6} \Pr^{1/3}$$

The assumptions for the model that will be used below are the followings:

1. ideal gas
2. heat, mass, and momentum transport in the radial direction of the column are neglected and only axial coordinate is considered
3. Knudsen and molecular diffusion is used as macro pore diffusivity
4. Film mass transfer in the layer surrounding the pellets is considered
5. void fraction is uniform in the entire column

4.7 MODEL ASSUMPTIONS

➤ The process is controlled by intracrystalline diffusion; mass transfer resistances associated with macro pore diffusion and film diffusion are neglected.

➤ Only two phases are considered, the bulk gas phase, and the solid phase.

➤ For the gas phase, the ideal gas law is assumed.

➤ The flow occurs only in axial direction (plug-flow with axial dispersion). No radial gradients are considered.

➤ The energy balance is included in the model, because the temperature change due to adiabatic compression / expansion as well as the heat of adsorption / desorption is significant.

➤ The momentum balance is described by the Ergun pressure drop equation (4.1), assuming quasi-stationary behaviour.

➤ The void fraction is uniform in the entire column.

4.8 MASS AND HEAT TRANSFER BALANCE

Gas-Solid Mass Transfer (O_2 diffuse to coked catalyst pores)

Gas Phase:

$$U_{og}C_{gi-1} = U_{og}C_{gi} + k_m\Delta x_i(1-\varepsilon)(S_p/V_p)(C_{gi} - C_{ps}) \quad \text{------------------------(1)}$$

Solid Phase:

$$k_m\Delta x_i(1-\varepsilon)(S_p/V_p)(C_{gi} - C_{ps}) = k_r\rho_p\Delta x_i(1-\varepsilon)C_{ps}\xi L_c \quad \text{--------------------- (2)}$$

Energy Balance

Gas-Solid Heat Transfer (O_2 diffuse to coked catalyst pores)

Gas phase:

$$U_{og}\rho_p C_{p,g}T_{gi-1} = U_{og}\rho_p C_{p,g}T_{gi} + h\Delta x_i(1-\varepsilon)(S_p/V_p)(T_{gi} - T_{ps}) \quad \text{------------(3)}$$

Solid Phase:

$$h\Delta x_i(1-\varepsilon)(S_p/V_p)(T_{gi} - T_{ps}) = (-\Delta H_r)k_r\rho_p\Delta x_i(1-\varepsilon)C_{ps}\xi L_c \quad \text{------------(4)}$$

4.8.1 GAS PHASE

The following assumptions have been made for simplicity of the model:

➤ Mass transfer resistance between the gas phase and the pellets occurs at infinitely fast rate, in consequence the concentration in the bulk gas and in the pores is considered to be the same, hence and the total bed void is used in the accumulation term.

➤ Mass transfer due to axial dispersion is limited to the bed void fraction.

➤ There is not inter - crystal mass transfer.

$$\varepsilon_T \frac{\partial C_i}{\partial t} = \frac{\partial (C_i u_g)}{\partial z} + \varepsilon_b C_T \frac{\partial}{\partial z}\left(D_{axi} \frac{\partial}{\partial z}\left(\frac{C_i}{C_T} \right) \right) - Ads_{rate}$$

Ads_{rate} adsorption rate

D_{ax} axial dispersion coefficient

C_i molar gas phase concentration

C_T total gas phase concentration

u_g superficial gas velocity

ε_b bed void fraction

ρ_b bed density

ε_T total bed porosity

4.8.2 ADSORPTION RATE

A linear driving force (LDF) is assumed for the mass transfer, crystalline resistance. The rate, modelled with this approach, appears as source term in both particle and gas balances, determined by: (see also Table 3.1)

$$Ads_{ratei} = \frac{15 \rho_b D_{ci}}{r_c^2}\left(q_{eqi} - q_i \right)$$

D_{ci} crystal diffusivity, as determined in section 3.4.3

r_c crystal radius

$q_{eq,i}$ equilibrium load of adsorbent

q_i given load of adsorbent material

ρ_b bed density

4.8.3 SOLID PHASE

The component conservation in the solid phase is defined as:

$$\rho_b \frac{\partial q_i}{\partial t} = Ads_{ratei}$$

The dynamic behaviour of the column is given by the solution of C(z,t), q(z,t), subject to the initial and boundary conditions. The response to a change in the feed composition involves a concentration front, which propagates through the column depending on the equilibrium isotherm (Ruthven, 1984; p. 221-222); dispersion and kinetics.

4.9 ENERGY BALANCE

The following assumptions and explanations are needed in order to understand the model for the energy balance adopted:

> The process considered is non-isothermal.

> The thermal axial dispersion term was described in analogy with the mass dispersion. Experimental measurements of fluid particle heat transfer, in general, confirm the validity of the analogy with mass transfer, especially at higher Reynolds numbers (Ruthven, 1984; p. 216).

> It was assumed that the heat transfer between the gas and adsorbed phases were extremely fast, producing no temperature difference between them.

> The system is considered to be adiabatic.

> The temperature is considered to be uniform within an individual adsorbent particle, which implies that the major resistance to heat transfer occurs in the external fluid film rather than within the particles (Ruthven, 1984; p. 217).

4.9.1 GAS PHASE ENERGY BALANCE

The overall and general heat balance contains terms for heat accumulation, thermal dispersion, heat transport due to convection, adiabatic polytrophic compression, heat transfer from gas to solid, heat transfer from gas to internal wall and heat of adsorption included in the solid energy balance.

The following assumptions have been made for simplicity:

➤ The accumulation term considers both, bulk gas phase and gas within the particles (total bed porosity). This implies that the gas temperature within the pores is the same as in the surrounding fluid.

➤ As explained in the axial temperature dispersion is described in analogy with axial concentration dispersion, therefore the bed void term multiplies the dispersion flux, indicating that thermal axial dispersion occurs only in the bulk phase.

Thus the resultant equation is:

$$\varepsilon_T \rho_g Cp_g \frac{\partial T_g}{\partial t} = \varepsilon_b \frac{\partial}{\partial z}\left(\lambda_{ax}\frac{\partial T_g}{\partial z}\right) - \rho_g Cp_g \frac{\partial(T_g u_g)}{\partial z} + \varepsilon_T R \frac{\partial P}{\partial t} - Q_{gs} - Q_w$$

Cp_g gas heat capacity

T_g gas phase temperature

P pressure

Q_{gs} heat exchange between gas and solid phase

Q_w heat exchange with the wall

R universal gas constant

ε_b bed porosity

ε_T total bed porosity

λ_{ax} effective gas thermal dispersion coefficient

λ_g gas thermal conductivity

ρ_g gas density

4.9.2 SOLID PHASE ENERGY BALANCE

The solid phase energy balance includes terms for accumulation of heat in the solid, accumulation of enthalpy in the adsorbed phase, heat of adsorption and the gas - solid heat transfer.

The energy balance for the solid phase is:

$$\left(Cp_S + \sum_{j=1}^{n} \left(q_j Cp_{l_j} Mw_j \right) \right) \rho_b \frac{\partial Ts}{\partial t} = Q_{gs} - Q_{ads}$$

Cp_S, Cp_l heat capacity of the adsorbent and fluid phase respectively

Q_{ads} heat of adsorption

4.9.3 HEAT OF ADSORPTION

The contribution of the heat of adsorption must be included in the model. The rate of heat generation by adsorption of each component is a function of the local rate mass transfer. Thus the following equation applies:

$$Q_{ads} = \rho_b \left(\sum_{j=1}^{n} \frac{\partial q_j}{\partial t} Hads_j \right)$$

$Hads_j$ adsorption enthalpy

H_{ads} is negative, therefore $-Q_{ads}$ is positive in case of adsorption $\left(\frac{\partial q_i}{\partial t} > 0 \right)$.

- 20 -

4.9.4 THERMAL EQUILIBRIUM BETWEEN GAS AND SOLID PHASE

The following assumptions are valid under conditions and they are used for simplicity:

> The gas transfer between the gas and the solid is infinitely fast, hence the temperature difference between these two phases is the same, $T_g = T_s = T$. Solving the solid energy balance for Q_{gs} and introducing the results in the gas energy balance yields a new transport equation for temperature.

> For industrial processes the column can be considered as adiabatic, therefore the heat exchange with the wall is zero.

$$\rho_g Cp_g \varepsilon_T \frac{\partial T}{\partial t} + u_g \rho_g Cp_g \frac{\partial}{\partial z}(T) + \rho_b \left(Cp_S + \sum_{j=1}^{n} \left(q_j Cp_{l,j} Mw_j \right) \right) \frac{\partial T}{\partial t} =$$

$$\varepsilon_b \frac{\partial}{\partial z} \left(\lambda_{effec} \frac{\partial T}{\partial z} \right) + \varepsilon_T R \frac{\partial P}{\partial t} - Q_{ads}$$

Table 2.0 shows the equations to describe the system.

Model Equations

Ideal Gas Law	$P = C_T RT$
Equilibrium	$q_{eq_i} = q_{max_i} K_{equi_i} \exp\left(\dfrac{-H_{adsi}}{RT}\right) C_i RT \left(1 - \displaystyle\sum_{j=1}^{n} \dfrac{q_{eq,j}}{q_{max,j}}\right)^{ai}$
Ergun Equation	$\dfrac{\partial P}{\partial z} = -\left(\dfrac{150(1-\varepsilon_b)^2}{d_p^{\,2}\varepsilon_b^{\,3}} \mu_g u_g + 1,75\rho_g \dfrac{(1-\varepsilon_b)}{d_p \varepsilon_b^{\,3}} u_g |u_g|\right)$
Mass Balance	$\varepsilon_T \dfrac{\partial C_i}{\partial t} = \dfrac{\partial(C_i u_g)}{\partial z} + \varepsilon_b C_T \dfrac{\partial}{\partial z}\left(D_{axi} \dfrac{\partial}{\partial z}\left(\dfrac{C_i}{C_T}\right)\right) - \rho_b \dfrac{\partial q}{\partial t}$
Adsorption Rate	$\dfrac{\partial q}{\partial t} = \dfrac{15 D_{ci}}{r_c^{\,2}}\left(q_{eqi} - q_i\right)$
Energy Balance	$\rho_g Cp_g \varepsilon_T \dfrac{\partial T}{\partial t} + \rho_g Cp_g u_g \dfrac{\partial T}{\partial z} + \rho_b\left(Cp_S + \displaystyle\sum_{j=1}^{n}\left(q_j Cp_{L,j} MW_j\right)\right)\dfrac{\partial T}{\partial t} =$ $\varepsilon_b \dfrac{\partial}{\partial z}\left(\lambda_{effec} \dfrac{\partial T}{\partial z}\right) + \varepsilon_T R \dfrac{\partial P}{\partial t} - Q_{ads}$
Heat of Adsorption	$Q_{ads} = \rho_b\left(\displaystyle\sum_{j=1}^{n} \dfrac{\partial q_j}{\partial t} Hads_j\right)$

CHAPTER 5

RESULT AND DISCUSSIONS
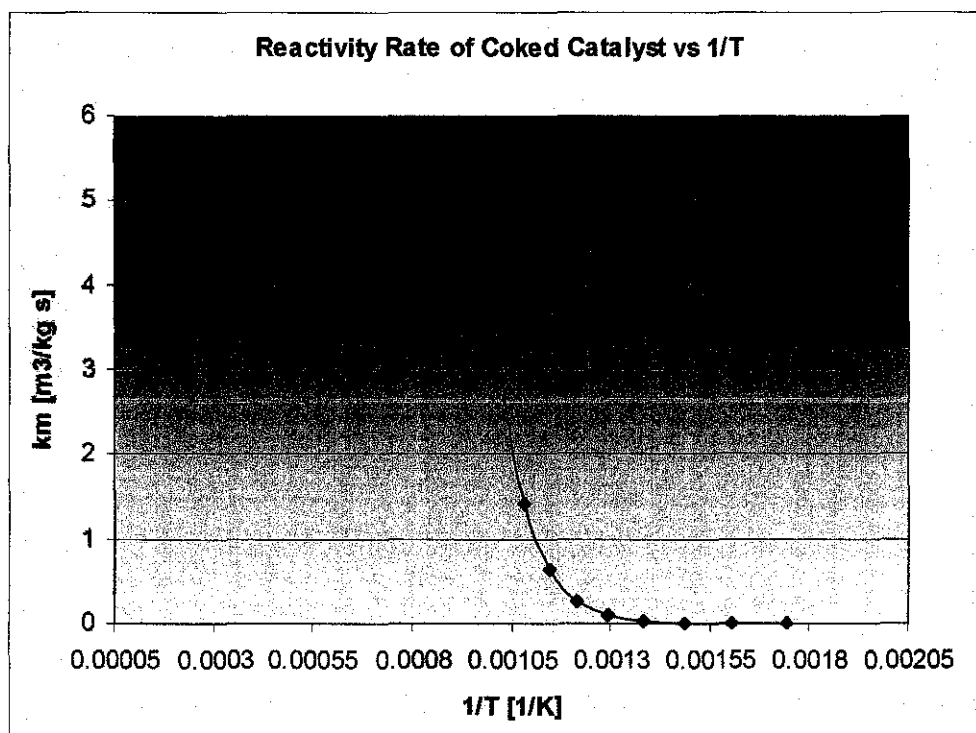
Figure 2.0 Reactivity rate of coked catalyst vs 1/T

Based on **Figure 2.0**, reactivity rate of fresh catalyst decreases exponentially with increase in surface temperature of the catalyst. This obviously showing, formation of coke is getting rapid with increase in the surface temperature of the catalyst. This temperature rise can be detected by placing thermocouples in the tubes where catalysts are placed. When temperature reaches at 550°C, coked catalyst then regenerated by burning off with mixture oxygen and nitrogen.
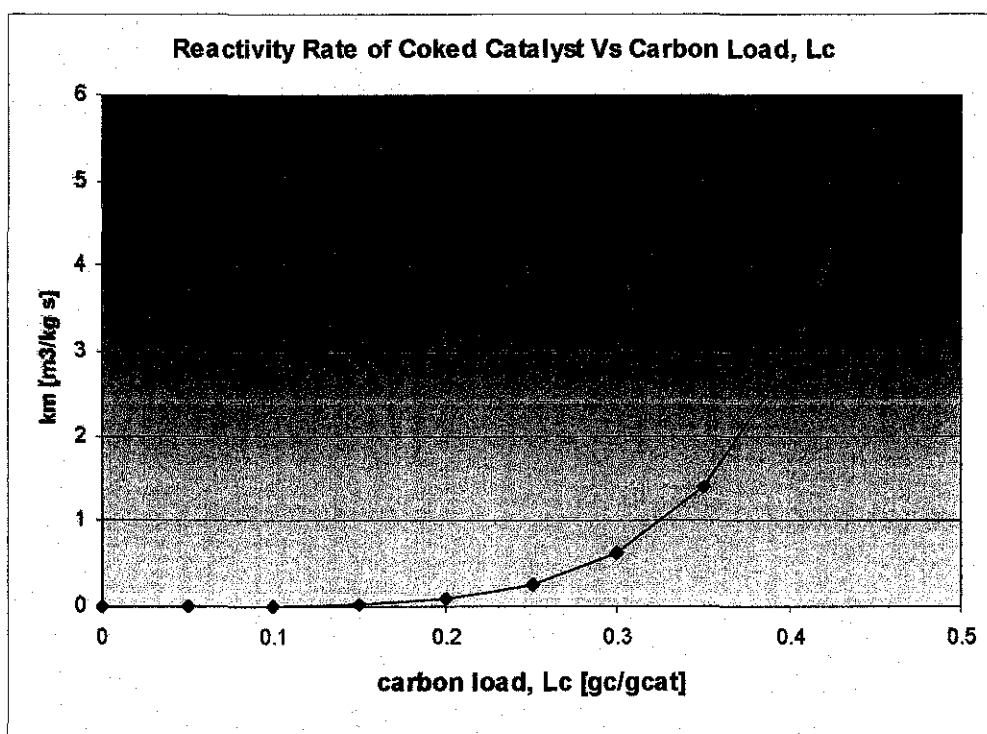
Figure 2.1 Reactivity rate of coked catalyst vs carbon load, Lc

Figure 2.1 shows reactivity rate of coked catalyst increase exponentially with increase in carbon load in the catalyst. We can see that influence of carbon load on the reaction rate, km is negligible at beginning of the process and then it increase gradually. This due to only one type of coke formed at the beginning and reaction rate gets more reactive than the coke on the acidic sites and rapidly burned off during the initial period of regeneration.
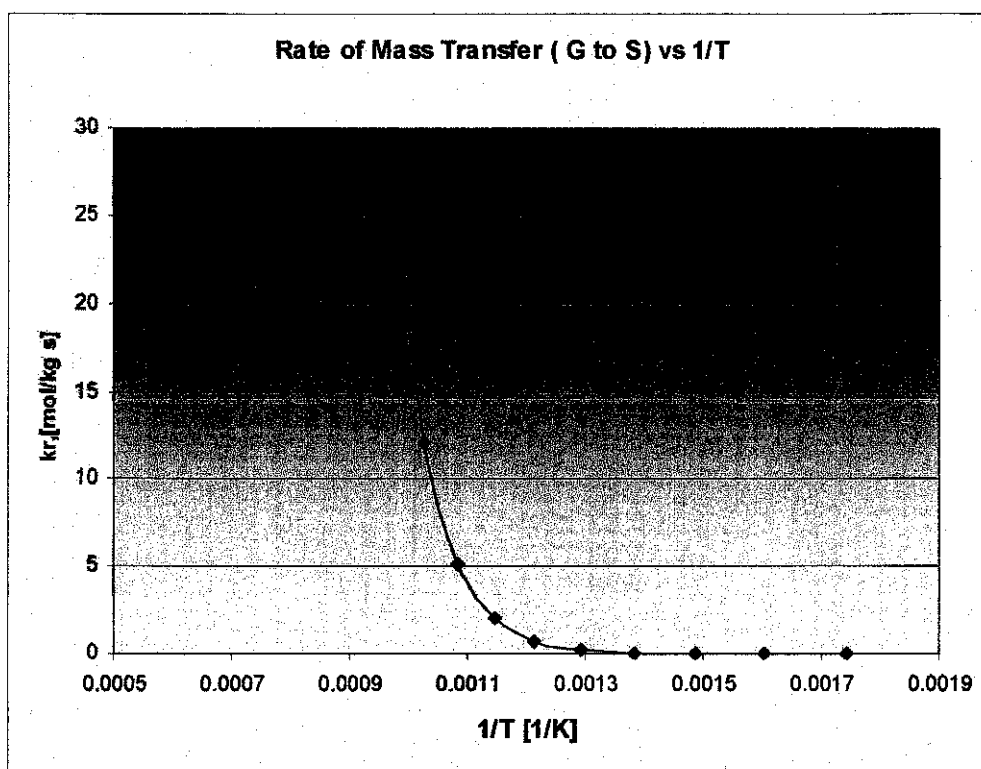
Figure 2.2 Rate of mass transfer from gas phase to solid phase vs 1/T

Figure 2.2 shows rate of mass transfer decreases exponentially with increase in the surface temperature of the catalyst. This is due to formation of coked getting active with the increase in the surface temperature. More carbon compound start to deposit on the active site of the catalyst pores. This can give a great impact on the catalyst structure, this can be proved by experiment (literature based) coked catalyst is regenerated for certain period of time with 0.3vol% O_2 in N_2 at 500 °C (in order to determine the rate of reaction, km) the coked catalyst was treated with pure N_2 and this part is repeated again with higher temperature at 750 °C(for 15 hours each). In case of a very high temperature during the treatment with N2 (750 °C) the reactivity decreases by a factor of about 6m, where as for the treatment at 500 °C has no effect on the coke structure and reactivity.
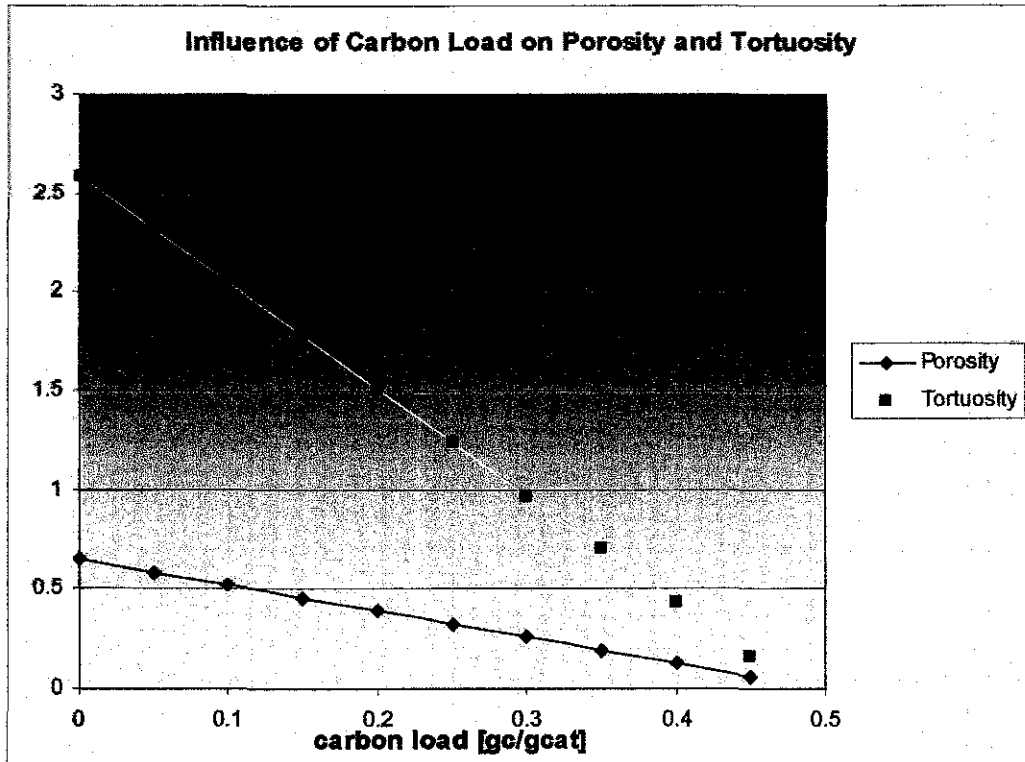
Figure 2.3 Influence of carbon load on porosity and tortuosity

Carbon load, Lc has strong influence on the tortuosity and porosity respectively based on **Figure 2.3**. Tortuosity and porosity decreases as the formation of carbon load increases. This is due to arise in coke deposited in the pore volume and internal surface of the catalyst. Entire fresh catalyst has higher values of ε_p and τ_p then coked catalyst. As the time goes, carbon will cover the surface layer of the pore volume of the catalyst and decreases the effectiveness of the catalyst reaction.
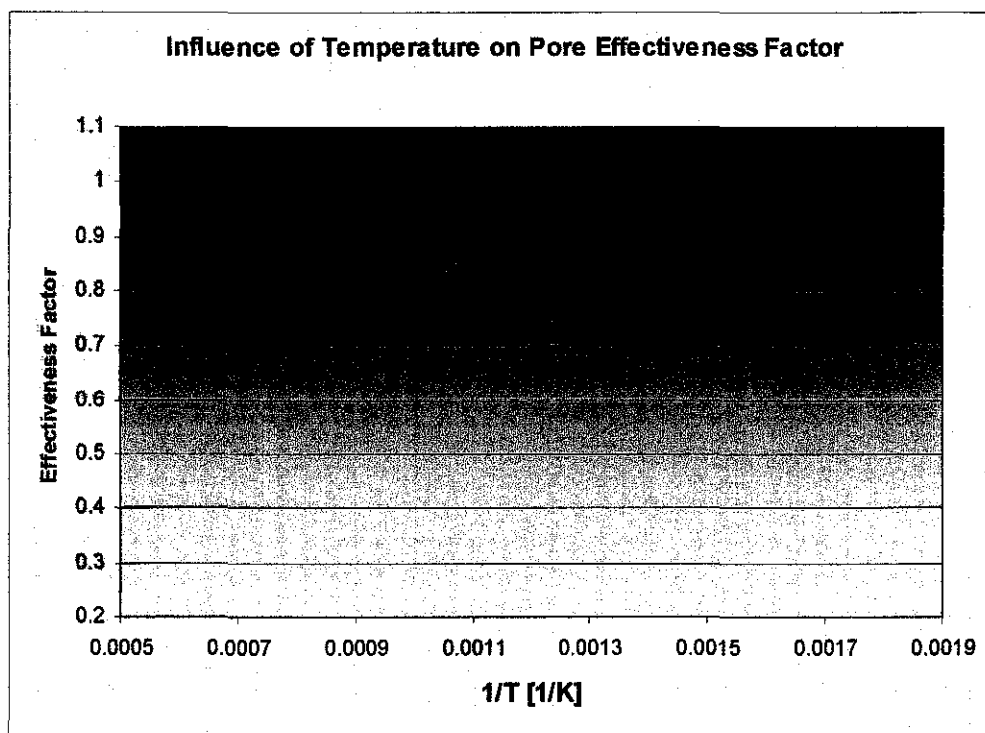
Figure 2.4 Influence of temperature on pore effectiveness factor

Pore effectiveness factor increases as there is arise in the surface temperature of the catalyst as show in **Figure 2.4**. We can see as the temperature rises till 500 °C, the effectiveness factor of the pore volume also increases. Above 500oC, the profile shows effectiveness factor become negligible through out the process. This clearly shows that formation of coke has started to clog the pore volumes and deactivated the active site of the catalyst.
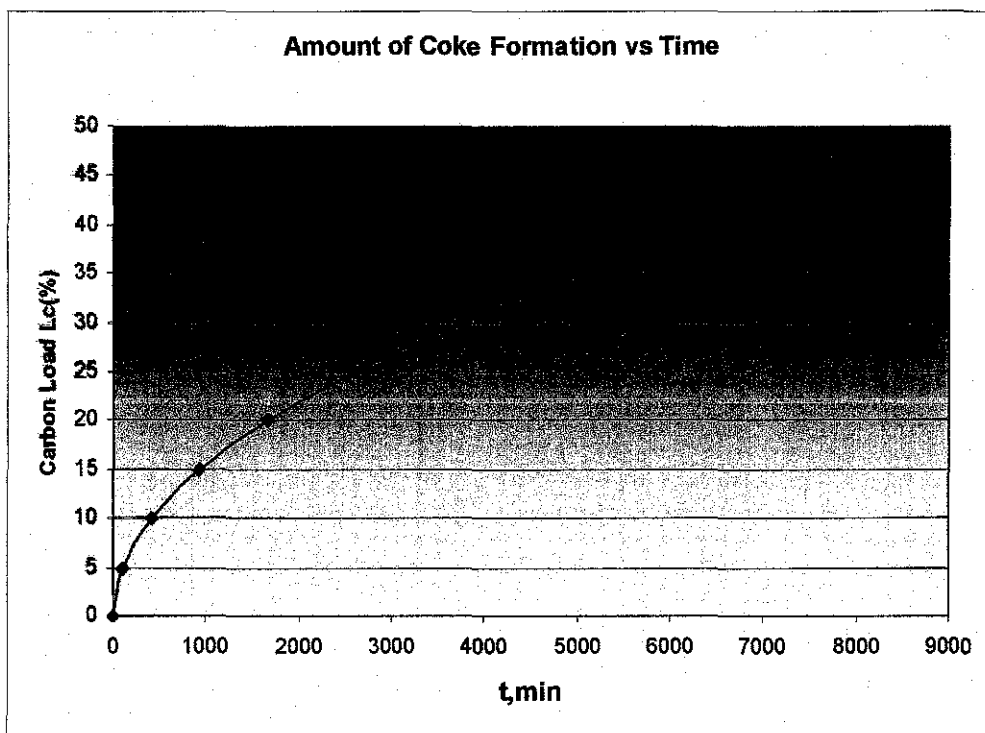
Figure 2.5 Amount of coke formation on time based

Based on **Figure 2.5**, we can see that formation of coke in a catalyst increases gradually with residence time. Percentage of carbon load shows the amount of coked formed on the catalyst through out the process. Based on literature, hydrogen strongly inhibits the rate of coke formation but has no influence on the reactivity of the carbonaceous deposits.
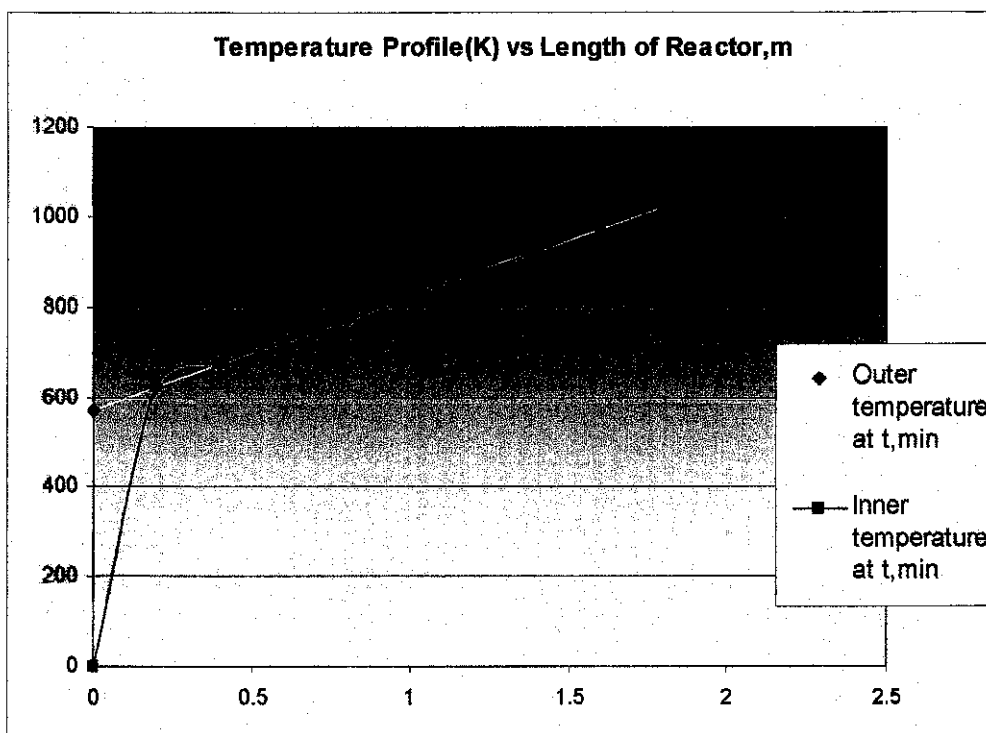
Figure 2.6 Temperature profile against length of reactor

Figure 2.6 shows the temperature profile of inner and outer temperature of the regeneration of coked catalyst. Inner temperature (final temperature) raises quickly until its reaches same as the outer temperature (initial temperature) of the catalyst. This shows the coke burn-off getting rapid by the increase of the temperature. More formation of carbon dioxide occurs.
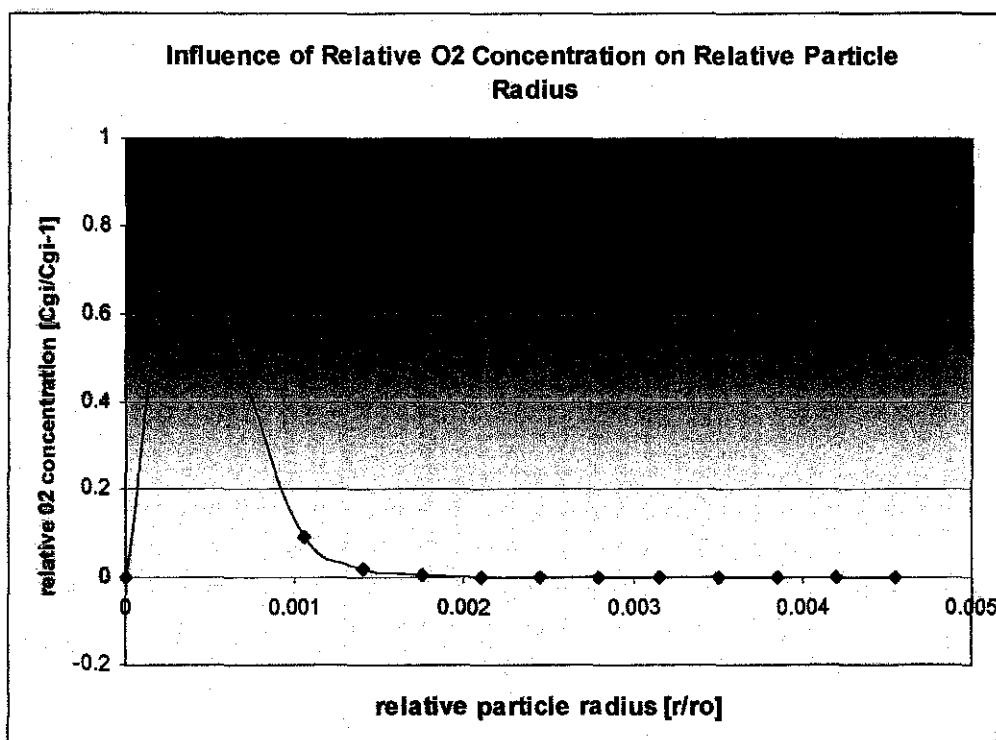
Figure 2.7 Influence of relative O_2 concentration on relative particle radius

Figure 2.7 shows the influence of relative O_2 concentration on relative catalyst particle radius. We can see that the relative O_2 concentration increases gradually until certain level of relative radius of the catalyst, and then it decreases exponentially. This clear because the O2 concentration start to penetrate and diffuse to the active site of the coked catalyst before it starts to burn of the carbon deposited on the catalyst. As more carbon burn-off takes place, relative concentration for O_2 decreases.
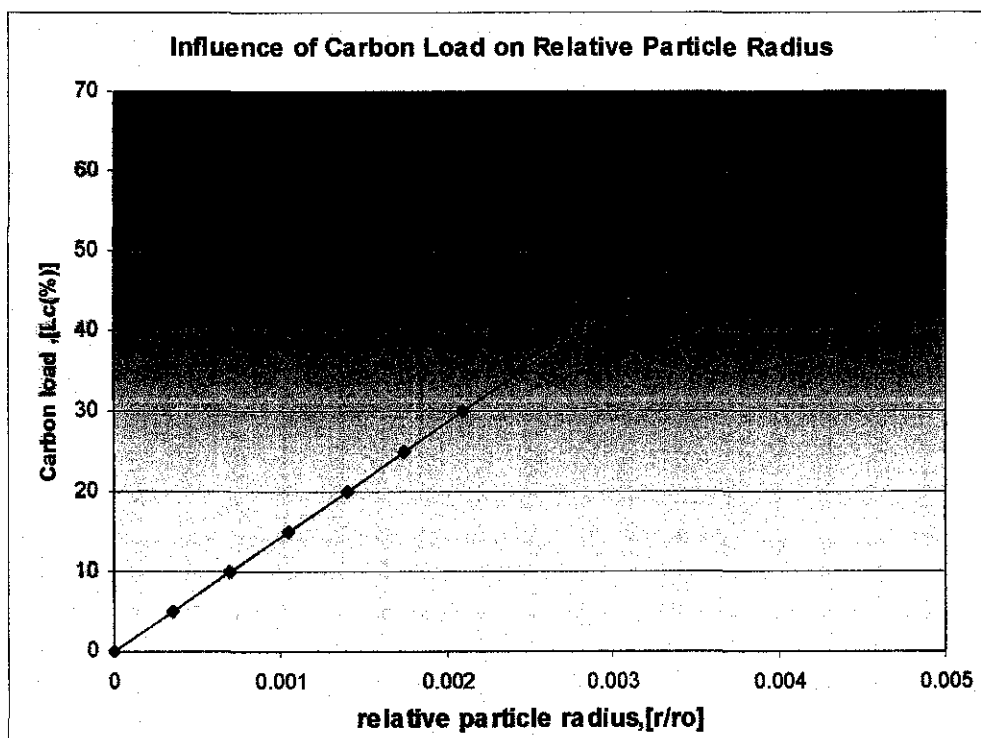
Figure 2.8 Influence of carbon load on relative particle radius

Figure 2.8 shows influence of the carbon load on relative particle radius. Percentage of carbon load increases gradually as the relative coked catalyst particle radius increases. This show the amount of coke deposit increases as the process takes place. Hence it reduces the active site of pore volumes of the catalyst, and as the process duration goes on catalyst will be deactivated and regeneration process must carry on before it liberate excess heat in the reactor and then spoil as well damage the catalyst structure.

CHAPTER 6

CONCLUSION & RECOMMENDATIONS

6.1 CONCLUSION

The present invention provides a process for removing coke deposits from particulate matter, and is particularly useful for regenerating coked catalyst used in petroleum processing operations. The process comprises a first step in which the particulate matter is heated by combusting a fuel with air in the presence of the particulate matter. The combustion produces a gaseous exhaust mixture comprised of nitrogen and carbon dioxide. The exhaust gas also usually contains small amounts of other impurities, such as sulphur oxides and nitrogen oxides. The exhaust gas exits the regenerator and is next introduced into a separating device wherein nitrogen is separated from the other components of the exhaust gas and discharged to the atmosphere, or otherwise disposed of. All or a portion of the remaining gas stream, which is comprised predominantly of carbon dioxide, is recycled to the reactor, with simultaneous introduction of oxygen into the reactor. As the volume of carbon dioxide and oxygen entering the reactor increases, the flow of air to the reactor is reduced. The relative amount of each gas entering the reactor is regulated to maintain the combustion rate at the desired level. Eventually, the desired degree of air replacement by oxygen and carbon dioxide recycle gas is attained; afterwards the amounts of oxygen and carbon dioxide, and perhaps air, introduced into the reactor are regulated to optimize the overall process.

The conversion from air operation to operation with oxygen and carbon dioxide may take place with the system already in operation with air being used as the source of

oxygen, or with the system being started cold. In the former case, the coke on the particulate matter will serve as fuel for the production of carbon dioxide. This embodiment can be practiced with batch or continuous processes. When the process is started cold, it can be initiated using fresh particulate matter or with equilibrium particulate matter, i.e. particulate matter from an earlier run which is clean or fouled with coke. In either case, a liquid or gaseous hydrocarbon fuel, such as fuel oil, can be used for the production of carbon dioxide and to heat the particulate matter to the desired operating temperature. When the temperature reaches the point at which the coke begins to burn, the use of fuel can be terminated and the process continued using the coke as fuel.

This embodiment is particularly suitable when the process is continuous, e.g. when the process is a fluidized catalytic reaction process with freshly regenerated catalyst being transferred from a catalyst regenerator to a cracking reactor and coked catalyst being transferred from the reactor to the regenerator. When the system reaches equilibrium, a mixture of oxygen and carbon dioxide, or oxygen, carbon dioxide and air (or other oxygen-inert gas mixtures) can be used to support the coke combustion step. Carbon dioxide can be separated from the lighter constituents by any suitable means, including adsorption, absorption, liquefaction, distillation or membrane separation. In a preferred embodiment, the separation is effected by pressure swing adsorption (PSA) using an adsorbent selected from silica gel, activated alumina, zeolites or mixtures of these, which preferentially adsorbs carbon dioxide over other constituents of the exhaust gas. In a most preferred embodiment the PSA separation uses silica gel adsorbent.

In another preferred embodiment, the particulate matter is a hydrocarbon cracking catalyst and the catalyst regeneration step is part of a continuous process comprising a catalytic hydrocarbon processing step in which the catalyst becomes fouled with coke, and a catalyst regeneration step, in which the coke deposits are burned off the coked catalyst.

6.2   RECOMMENDATIONS

Laboratory experimental work should be carried up to verify and as well to justify the modeling of regeneration of the coked catalyst in future.

REFERENCE

> *Chemical Engineering Science, Volume 60, Issue 15, August 2005, Pages 4249-4264* Christoph Kern, Andreas Jess

> Liang et al. / J Zhejiang Univ SCI *A Study On Naphtha Catalytic Reforming Reactor*

> Smith, R.B., 1959. Kinetic analysis of naphtha reforming with platinum catalyst. Chem. Eng. Progr., 55(6):76-80.

> LEVENSPIEL, Octave. **Chemical Reaction Engineering.** Second Edition, John Wiley & Sons. USA, 1972.

> BIRD BYRON. **Transport Phenomena.** John Wiley & Sons. United States of America. 2002.

> Mathematical Model for a Pressure Swing Adsorption Process, Tahnee González Martínez

> RUTHVEN, Douglas. **Principles of Adsorption and Adsorption Processes.** John Wiley and Sons. University of New Brunswick. Canada. 1984.

> ULLMANS. **Processes and Process Engineering.** Volume 1 Separation Processes. Wiley VCH. 1999 Germany.

> \VILLADSEN, John. **Solution of differential equation models by polynomial approximation.** Prentice Hall, USA. 1978.

APPENDIX A

Gas-Solid Mass Transfer (O_2 diffuse to coked catalyst pores)

Equation created based on literature review,

$$U_{og}C_{gi-1} = U_{og}C_{gi} + k_m\Delta x_i(1-\varepsilon)(S_p/V_p)(C_{gi} - C_{ps}) \text{------------------------}(1)$$

$$k_m\Delta x_i(1-\varepsilon)(S_p/V_p)(C_{gi} - C_{ps}) = k_r\rho_p\Delta x_i(1-\varepsilon)C_{ps}\xi L_c \text{----------------------}(2)$$

> Finding C_{ps} from equation 2
> Eliminate C_{ps} by substituting into the equation 1
> Final form of gas-solid mass transfer equation in term of (C_{gi-1}/ C_{gi}) to be obtained

$$\frac{Cgi - 1}{Cgi} = 1 + \frac{\dfrac{\Delta x_i(1 - \varepsilon)}{Uog}}{\dfrac{1}{k_r\rho_p\xi L_c} + \dfrac{V_p}{k_m S_p}}$$

Gas-Solid Heat Transfer (O_2 diffuse to coked catalyst pores)

Equation created based on literature review,

$$U_{og}\rho_p C_{p,g}T_{gi-1} = U_{og}\rho_p C_{p,g}T_{gi} + h\Delta x_i(1-\varepsilon)(S_p/V_p)(T_{gi} - T_{ps}) \text{-------------}(3)$$

$$h\Delta x_i(1-\varepsilon)(S_p/V_p)(T_{gi} - T_{ps}) = (-\Delta H_r)k_r\rho_p\Delta x_i(1-\varepsilon)C_{ps}\xi L_c \text{-------------}(4)$$

> Finding T_{ps} from equation 3
> Eliminate T_{ps} by substituting into the equation 4
> Final form of gas-solid heat transfer equation in term of (T_{gi-1}/ T_{gi}) to be obtained

$$\left(T_{gi-1} - T_{gi}\right) = \frac{\left(-\Delta H_r\right)\Delta x_i (1-\varepsilon)C_{gi}}{U_{og}C_{p,g}\left[\dfrac{1}{\xi L_c k_r} + \dfrac{\rho_p V_p}{k_m S_p}\right]}$$

Where, r_o

$$\xi = \frac{1}{1 + M_T} \; ; \; M_T = \frac{D_p}{6}\sqrt{\frac{k_r L_c \rho_p}{D_{o2eff}}}$$

$$D_{O2eff} = \frac{\varepsilon_p}{\tau_p}\left(D_{O2,\,pore}\right) = \frac{\varepsilon_p / \tau_p}{\dfrac{1}{D_{O2,mol}} + \dfrac{1}{D_{O2,\,Knu}}} \; ;$$

$$D_{O2,\,Knu} = \frac{d_{pore}}{3}\sqrt{\frac{8RT}{\pi M_{O2}}}$$

$$S_p = \frac{Vp}{M_T}\sqrt{\frac{k_r}{D_{O2,eff}}} \; ; \; t,\min = \left(\frac{Lc(\%)}{0.49}\right)^2 \; ;$$

$$k_r = \left(k_{m,C_0}e^{\frac{-E_A}{RT}}\right)L_c C_{O_2}$$

APPENDIX B

NOMENCLATURE

ξ	pore effective factor
U_{og}	interstitial gas velocity (ms^{-1})
C_{gi-1}	concentration of gas at i-1 position (mol/m^3)
C_{gi}	concentration of gas at i position (mol/m^3)
ρ_p	density of catalyst (kg/m$_3$)
ρ	density of gas (kg/m^3)
$C_{p,g}$	heat capacity of gas phase (J/mol K)
T_{gi-1}	Temperature of gas at i-1 position (K)
T_{gi}	Temperature of gas at I position (K)
H	heat capacity of solid phase (J/mol K)
Δx_i	thickness
ε	voidage of bed
ε_p	porosity of catalyst particle
τ_p	particle tortuosity
M_{O2}	molecular weight of oxygen (kg/mol)
d_p	diameter of the catalyst, (m)
S_p	surface reaction of catalyst
V_p	volume of catalyst (m^3)
T_{ps}	temperature at surface of catalyst particle
$(-\Delta H_r)$	heat of reaction, (J/Mol)
k_r	rate of mass transfer from gas to solid
C_{ps}	concentration at catalyst surface
L_c	Carbon load of catalyst, kg$_c$ / kg$_{catalyst\ load}$
k_m	rate of reaction at C_{gi} and catalyst surface, m^3/kg s
M_T	mass transfer coefficient
$D_{O2,eff}$	effective diffusion coefficient, m^2/s
$D_{O2,Knu}$	Knudsen diffusion coefficient, m^2/s
d_{pore}	diameter of the catalyst pore
ΔT_{ad}	adiabatic temperature different ($^{\circ}$C)

Subscripts

b	bed
g	gas phase
i	component i
j	component j
l	liquid phase
s	solid phase
T	total
w	wall
∞	Environment

Latin symbols

a		number of neighbouring sites occupied
a_{ax}	m²/s	thermal dispersion coefficient
a_{td}	m²/s	thermal diffusivity
A	m²	bed cross sectional area
Ads_{rate}	mol/m³s	adsorption rate
A_{sp}	m²/m³	macroscopic particle surface per bed volume
A^0	kJ/mol	reference adsorption potential
C	mol/m³	gas phase concentration
Cp	J/kgK	gas heat capacity
d_{ext}	m	extrudate diameter
d_{in}	m	internal diameter of the column
d_p	m	equivalent pore diameter
D_{ax}	m²/s	axial dispersion coefficient
D_o	m²/s	crystal diffusivity
D_c^∞	m²/s	infinite dilution crystal diffusivity
D_{c0}^∞	m²/s	infinite dilution crystal diffusivity at infinite temperature
Des_{rate}	mol/m³s	desorption rate
D_k	m²/s	Knudsen diffusivity
D_m	m²/s	molecular diffusivity
D_p	m²/s	pore diffusivity
e	m	thickness of the column wall
Ea	J/mol	activation energy
E_0	kJ/mol	characteristic energy
g	m/s²	gravity acceleration, (9,81 m²/s)
H_{ads}	J/mol	heat of adsorption of component i
J		molar flux
k	J/K	Boltzmann constant
kl	m³s/mol	adsorption rate constant
k_f	s⁻¹	film mass transfer coefficient
k_{fe}	m/s	external mass transfer coefficient,
k_g	W/m²K	film heat transfer resistance coefficient between the gas phase and the column wall
$k_{g'}$	W/m²K	internal convective heat transfer coefficient
k_r		rate coefficient
k^∞	W/m²K	film heat transfer resistance coefficient between the column wall and the environment
k'_∞	W/m²K	external convective heat transfer coefficient
K_{eq}	1/Pa	equilibrium constant a given temperature
K_{eq}^0	1/Pa	adsorption equilibrium constant at reference temperature
L	m	bed length
L_{ext}	m	extrudate length
m	kg	mass
m_f		Freundlich exponent
Mw	kg/mol	molecular weight
P	Pa	pressure
Ps	mbar	saturation pressure
P^0	Pa	reference pressure
q	mol/kg	molar load of component
q_{eq}	mol/kg	equilibrium molar load
q_{max}	mol/kg	saturation capacity
q^0	mol/kg	load at reference state
Q_{ads}	W/m³	heat of adsorption
Q_{gs}	W/m³	heat transfer between gas and solid
r_c	m	crystal radius

r_p	m	particle radius
R	J/molK	ideal gas constant, (8,314 J/molK)
S		molecule
S_{ext}	m²	surface extrudate
t	s	time
T	K	temperature
u_g	m/s	superficial gas velocity
V_{ext}	m³	extrudate volume
x	-	mole fraction in the adsorbed phase
y	-	gas phase mol fraction

Greek symbols

α_{gs}	W/m²K	heat transfer coefficient between solid and gas
αgw	W/m²K	heat transfer coefficient between gas and column wall
α_p	kg/m³s	Ergun equation parameter
β	1/K	thermal expansion coefficient
β_p	kg/m⁴	Ergun equation parameter
ε	K	Lennard-Jones force constant
ε_b	-	bed void
ε_p	-	particle void
ε_T	-	total bed void
φ	kJ/mol	modified spreading pressure
λ	W/mK	thermal conductivity
λ_{ax}	W/mK	effective axial thermal conductivity
λ_{effe}	W/m	effective gas thermal dispersion coefficient
μ	Pa.s	dynamic viscosity
θ	-	Fractional coverage of adsorbed component on adsorbed phase
ρ	kg/m³	bed density
σ	Å	collision diameter from the Lennard Jones potential
$\Omega_{D,ij}$		collision integral for diffusion, a function of ε/KT
τ		tortuosity factor
ν	m²/s	kinematic viscosity

Dimensionless numbers

$$Nu = \frac{\alpha_{gs_x} d_p}{\lambda_g}$$

Nusselt

$$Pe = \frac{u_g d_p}{D_{ax}}$$

Peclet

$$Pr = \frac{C_{pg} \mu_g}{\lambda_g}$$

Prandtl

$$Ra = Gr\,Pr = \frac{g\beta(T_w - T\infty)L^3}{\nu \times a}$$

Rayleigh

$$Re = \frac{\rho_g u_g d_p}{\mu_g}$$

Reynolds

$$Sh_i = \frac{k_{fi}d_p}{D_{m,i}} \qquad \text{Sherwood}$$

$$Sc_i = \frac{\mu_g}{\rho_g D_{mi}} \qquad \text{Schmidt}$$

APPENDIX C

Length, Z (m)	Carbon Load,(L_c)	Porosity (ε_p)	Tortuosity (τ_p)	Rate of Reaction (k_m)	Initial Temperature (Tgi-1)	Rate of Mass Transfer (k_r)	Initial Concentration ,Cgi-1 (mol/m3)
0	0	0.65	2.59	0.000283581	573.15	0	10.5
0.2	0.05	0.585	2.32	0.001718338	623.15	0.003608273	10.49931158
0.4	0.1	0.52	2.05	0.007967199	673.15	0.033460043	10.49931158
0.6	0.15	0.455	1.78	0.029879852	723.15	0.188230726	10.49931158
0.8	0.2	0.39	1.51	0.094449584	773.15	0.793324491	10.49931157
1	0.25	0.325	1.24	0.259597832	823.15	2.725598521	10.49931157
1.2	0.3	0.26	0.97	0.635495929	873.15	8.006723713	10.49931157
1.4	0.35	0.195	0.7	1.411908491	923.15	20.75369402	10.49931157
1.6	0.4	0.13	0.43	2.889843961	973.15	48.54619539	10.49931156
1.8	0.45	0.065	0.16	5.51492081	1023.15	104.2251693	10.49931156
2	0.28	0.0032	0.11	2.983747465	1073.15	208.0854036	10.49931156

$D_{O2,Knu}$	$d_{pore(nm)}$	$D_{O2,eff}$	Mass Transfer Coefficient (M_D)	pore effective factor, ξ	Surface Reaction Rate ,S_p	Cgi(mol/m3)	ΔTad	ΔH_r
48.02809773	7.4	0.053879095	0	1	0.001255670	9.999999999	246.30542	11259.676
43.65012904	6.45	0.054110296	0.000810126	0.99919053	0.003187552	9.876188106	197.04433	9008.3316
38.68549267	5.5	0.054398585	0.003479582	0.996532483	0.00225394	4.84501694	147.78325	6756.2487
33.17073613	4.55	0.054768322	0.01007358	0.990026885	0.001840334	0.973651436	98.522167	4504.1658
27.13712896	3.6	0.055258926	0.023773706	0.976778359	0.001593776	0.190059756	49.261084	2252.0829
20.61175078	2.65	0.05593631	0.048967926	0.953317995	0.001425517	0.045978827	0	0
13.61829909	1.7	0.056902405	0.091154982	0.916460097	0.001301313	0.013609855	49.261084	2252.0829
6.177701474	0.75	0.058047988	0.156944396	0.864345775	0.001204782	0.004775958	98.522167	4504.1658
4.78643212	0.40	0.074724113	0.22616994	0.815547639	0.00112697	0.001893951	147.78325	6756.2487
2.09383744	0.22	0.0895448	0.321092415	0.756949316	0.001062517	0.000844942	197.04433	9008.3317
0.12342483	0.07	0.037177067	1.066213336	0.48397713	0.000961083	0.000000432	246.30542	11260.415

T_{gi}	Cgi/Cgi-1	Xi,conversion	t, min	Lc(%)	r/ro
600.232443	0.999433	0.000343311	0	0	0
623.147229	0.940651	0.059348984	104.1233	5	0.00035
673.12943	0.4614604	0.53853956	416.4931	10	0.0007
723.092001	0.0927348	0.907265212	937.1095	15	0.00105
773.060695	0.0181021	0.981897884	1665.973	20	0.0014
823.155043	0.0043792	0.995620777	2603.082	25	0.00175
873.680235	0.0012963	0.998703738	3748.438	30	0.0021
925.362737	0.0004549	0.999545117	5102.041	35	0.00245
979.562246	0.0001804	0.999819612	6663.89	40	0.0028
1038.62003	8.048E-05	0.999919524	8433.986	45	0.00315
1052.34299	6.320E-06	0.99994843	10412.33	50	0.0035

Assumed to be constant through out the process:

U_0(m/s)	5
Δx_i	0.2
ε	0.4
ρ_p	1400 kg/m^3
V_p	0.00002
Dp	0.0045 m